Article

pubs.acs.org/Biomac

Electrically Conductive Chitosan/Carbon Scaffolds for Cardiac Tissue Engineering

Ana M. Martins,[†,‡,§] George Eng,[†] Sofia G. Caridade,[‡,§] João F. Mano,[‡,§] Rui L. Reis,[‡,§] and Gordana Vunjak-Novakovic*[,†]

[†]Department of Biomedical Engineering, Columbia University, New York, New York 10032, United States

[‡]3B's Research Group - Biomaterials, Biodegradables and Biomimetics, University of Minho, Guimarães, Portugal

[§]ICVS/3B's-PT Government Associate Laboratory, Braga/Guimarães, Portugal

ABSTRACT: In this work, carbon nanofibers were used as doping material to develop a highly conductive chitosan-based composite. Scaffolds based on chitosan only and chitosan/carbon composites were prepared by precipitation. Carbon nanofibers were homogeneously dispersed throughout the chitosan matrix, and the composite scaffold was highly porous with fully interconnected pores. Chitosan/carbon scaffolds had an elastic modulus of 28.1 ± 3.3 KPa, similar to that measured for rat myocardium, and excellent electrical properties, with a conductivity of 0.25 ± 0.09 S/m. The scaffolds were seeded with neonatal rat heart cells and cultured for up to 14 days, without electrical stimulation. After 14 days of culture, the scaffold pores throughout the construct volume were filled with cells. The metabolic activity of cells in chitosan/carbon constructs was significantly higher as compared to cells in chitosan scaffolds. The incorporation of carbon nanofibers also led to increased expression of cardiac-specific genes involved in muscle contraction and electrical coupling. This study demonstrates that the incorporation of carbon nanofibers into porous chitosan scaffolds improved the properties of cardiac tissue constructs, presumably through enhanced transmission of electrical signals between the cells.

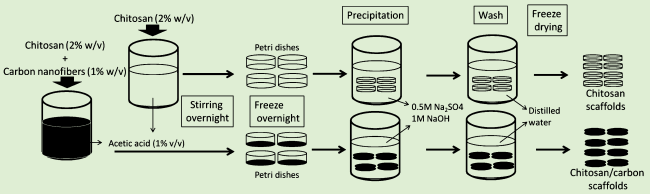

INTRODUCTION

Cardiac muscle is an electroactive tissue capable of transferring electrical signals and allowing the heart to beat. When damaged, adult heart muscle has poor capability to repair itself due to a minimal regeneration potential of cardiomyocytes.[1] In the past decade, great interest has arisen from the possibility to regenerate lost tissue by implanting therapeutic cells, biomaterials, and cardiac patches. Selection of a scaffold with appropriate mechanical and electrical properties is critical for inducing functional cardiac tissue, in vitro or in vivo.[2]

Several natural-based scaffolds have been proposed for cardiac applications[3−8] and studied with cells with the application of mechanical[5] and electrical stimulation.[9−12] The development of conductive materials for cardiac regeneration was also reported.[7,11,13−17] Chitosan is a suitable functional biomaterial because it is biocompatible, biodegradable, minimally immunogenic, nontoxic, and hydrophilic.[18−21] In addition, chitosan is a hemostatic agent,[22,23] with antithrombogenic properties.[24] Chitosan also has utility for drug delivery due to its nontoxicity, highly cohesive and hydrophilic properties, and polycationic character resulting from primary amine groups, providing high charge density in acidic solutions (pH < 6.5).[25,26] Chitosan is soluble in dilute or weak acids (such as acetic and formic acid), but it is normally insoluble in aqueous solutions above pH 6.5. In previous studies, chitosan hydrogel alone improved heart function by increasing neovascularization.[27−29]

Chitosan-based composites can combine several properties of interest to cardiac tissue engineering, including the natural-based origin and biodegradability (like collagen scaffolds) with adequate mechanical properties and electrical conduction. Since chitosan is nonconductive, its electrical properties could be improved by adding conductive material. We selected carbon nanofibers over carbon nanotubes for two reasons. Carbon fibers are larger in size and therefore easier to incorporate into chitosan. Also, carbon nanofibers have more sites on the outer wall than carbon nanotubes, which can facilitate the electron transfer of electroactive analytes, such as proteins or enzymes.[14,15,17]

Carbon nanofibers have ability to reinforce polymer scaffolds and produce excellent mechanical properties.[32] Also, carbon nanostructures have been considered as reinforcing filler for biological matrices to improve multiple functions, including electrical conductivity. Chitosan has been reinforced with carbon nanotubes to form various types of composites for biological applications,[33,34] but this material was never investigated for cardiac tissue engineering.

We hypothesized that electrically conductive scaffolds would improve cardiomyocyte function by increasing expression of cardiac genes, even without electrical stimulation. Our strategy was to combine the biocompatibility and biodegradability of

Received: November 13, 2013
Revised: January 10, 2014
Published: January 13, 2014

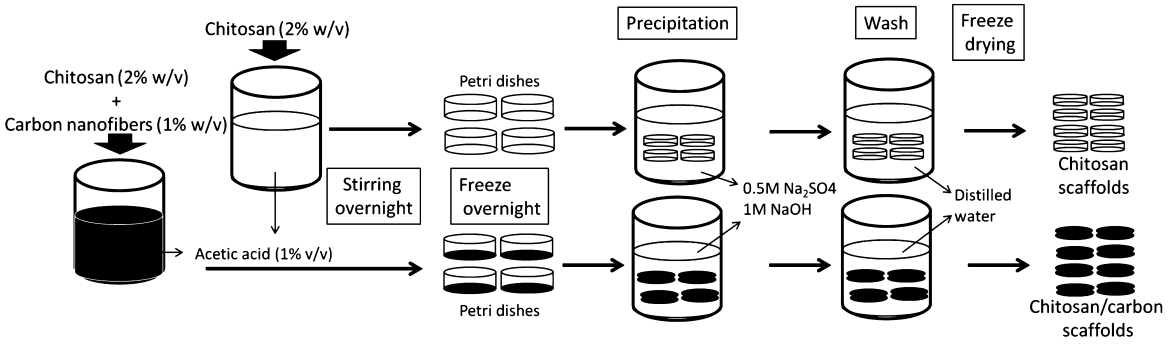

Figure 1. Scaffold preparation. Chitosan scaffolds were prepared using a 2% (w/v) solution of chitosan in 1% (v/v) acetic acid. An additional 1% carbon (w/v) was dispersed in the solution to make chitosan/carbon scaffolds. The solutions were casted into Petri dishes, frozen (−20 °C) overnight and immersed in a precipitation solution containing 25% (v) NaOH 1 M and 75% (v) Na_2SO_4 0.5 M. The resulting scaffolds were washed with distilled water and lyophilized.

chitosan with the electrical properties of carbon nanofibers. By seeding neonatal cardiomyocytes into chitosan/carbon scaffolds in the absence of electrical stimulation we investigated the following questions: (*i*) Are chitosan/carbon scaffolds adequate materials for cardiac applications, in terms of their mechanical and electrical properties? (*ii*) Is the integrity of chitosan/carbon scaffolds maintained over time in culture? (*iii*) What are the effects of carbon nanofibers on metabolic activity of cultured cardiomyocytes and the expression of cardiac genes? In this initial study, we found that chitosan/carbon scaffolds support the cultivation of cardiomyocytes over a period of two weeks, with increased metabolic activity and pronounced expression of specific cardiac genes associated with contraction and the conduction of electrical signals.

EXPERIMENTAL SECTION

Scaffold Preparation. The precipitation method[18,20] was used to prepare scaffolds containing either 2% chitosan (w/v) or 2% chitosan (w/v) and 1% carbon nanofibers (w/v). All reagents were purchased from Sigma (St. Louis, MO) unless otherwise specified. Briefly, chitosan was dissolved in 1% (v/v) acetic acid to obtain a 2% (w/v) solution. Another formulation was prepared from a solution containing 2% chitosan (w/v) and 1% carbon nanofibers (w/v; Cat. 719781, graphitized (iron-free), composed of conical platelets, $D \times L$ = 100 nm × 20−200 μm; w/v). The chitosan solution and chitosan/carbon dispersion were cast into Petri dishes and frozen immediately at −20 °C, a temperature that was maintained for 12 h.[18] They were then immersed in a precipitation solution that was formed by mixing 25% (v/v) of 1 M NaOH and 75% (v/v) of 0.5 M Na_2SO_4). After 12 h, the scaffolds were washed extensively with distilled water, and lyophilized (Figure 1). Scaffolds were die-punched into 6 mm diameter × 1.5 mm thick discs.

The scaffolds (n = 3 per group) were analyzed using micro-Computed Tomography (μCT) Skyscan 1072 (Skyscan, Kontich, Belgium). The X-ray was acquired with a pixel size resolution of 6.59 μm, and at X-ray source settings of 40 keV and 250 μA. The data sets were acquired over a rotation range of 180° (0.45° rotation step) and reconstructed using NRecon v1.4.3, SkyScan software. Representative data sets were segmented with a dynamic threshold of 40−255 and were used for morphometric analysis (CT Analyzer, v1.5.1.5, SkyScan) and to build the three-dimensional (3D) models (ANT 3D creator, v2.4, SkyScan).

The scaffold porosity, pore interconnectivity, pore size, and fiber thickness were measured. 3D virtual models of representative regions in the bulk of the scaffolds were created, visualized and registered using two image processing software packages, to access morphological changes (CT Analyzer and ANT 3D creator).

The interconnectivity was quantified as the accessible void fraction over a range of minimum connection sizes using an analysis software tool (CT Analyzer, v1.5.1.5, SkyScan). A 3D shrink-wrap process was performed to shrink the outside boundary of the volume of interest (VOI) in a scaffold through any openings whose size was equal to or larger than ∼50 μm. Any pores with the size below this value were considered to be closed. The interconnectivity was calculated as follows:

$$\text{interconnectivity} = (V_t - V_{sw})/(V_t - V_m) \times 100\%$$

where V_t is the total volume of the VOI, V_{sw} is the VOI volume after 3D shrink-wrap processing, and V_m is the volume of scaffold material.

Mechanical Testing. The dynamic viscoelastic measurements of hydrated scaffolds were performed using a TRITEC8000B Dynamic Mechanical Analysis (DMA) from Triton Technology (U.K.), in the dynamic compression mode. The scaffolds (6 mm diameter × 4 mm thick discs, n = 3 samples for each condition) were hydrated in phosphate buffered saline PBS solution overnight (5 mL PBS per scaffold, at room temperature). The experiments were performed under constant strain amplitude (50 μm). The elastic modulus (E') and the loss factor (tan δ) were measured in a frequency range of 0.1−10 Hz, at 37 °C. Elastic/storage modulus (E'), a measure of scaffold stiffness, was calculated as a function of frequency, and the two scaffolds were compared at 1 Hz. The loss factor (tan δ), a measure of the damping capability of a material, was also calculated as a function of frequency.

Degradation Studies. Degradation studies were performed by incubating the chitosan and chitosan/carbon scaffolds (n = 3 per group and time point) in phosphate buffered saline (PBS, pH 7.4) under static and dynamic conditions (agitation at 60 rpm) for up to 60 days. At each time point, the samples were removed, weighted for determination of water uptake, and dried for calculation of the weight loss.

Electrical Conductivity. The electrical conductivity of the dry and hydrated scaffolds was measured at room temperature using a Keithley 487 Picoammeter−Voltage source. The voltage was varied from −0.01 to 0.01 V, in steps of 0.001 V at 1 s intervals, and the current was measured within a Faraday cage, to avoid electromagnetic field interference. The volume resistivity (ρ) was then calculated from the characteristic $I-V$ curves by taking into account the geometrical characteristics of the sample:

$$\rho = V \times A/I \times L$$

where V is the applied voltage, I is the measured current, A is the area of the electrodes, and L is the distance between electrodes, corresponding to the thickness of the sample. In the present case the area was 19.6×10^{-6} m^2 and the sample thickness was 3−4 mm.

Electrical conductivity (σ) was then calculated as the inverse of the resistivity (ρ):

$$\sigma = 1/\rho$$

Culture of Neonatal Rat Cardiomyocytes. Neonatal rat cardiomyocytes were isolated from 2 day old Sprague−Dawley rats

dx.doi.org/10.1021/bm401679q | Biomacromolecules 2014, 15, 635−643

Table 1. Scaffold Properties

	chitosan	chitosan/carbon	method	samples
porosity (%)	91.5 ± 0.98	84.3 ± 7.6	μCT	$n = 3$
pore interconnectivity (%)	96.9 ± 1.3	96.2 ± 2.2	μCT	$n = 3$
pore size (nm)	149.7 ± 30.0	117.9 ± 5.62	μCT	$n = 3$
elastic modulus (kPa)	17.8 ± 4.6[a]	28.1 ± 3.3[a]	DMA	$n = 3$
conductivity (S/m; dry)	$7.4 \times 10^{-09} \pm 1.0 \times 10^{-09}$	0.25 ± 0.09	4-probe[b]	$n = 3$
conductivity (S/m; hydrated)	0.03 ± 0.02	0.04 ± 0.02	4-probe[b]	$n = 3$

[a]A significant difference ($p < 0.01$) was found between both conditions. [b]4-Probe: four-probe method.

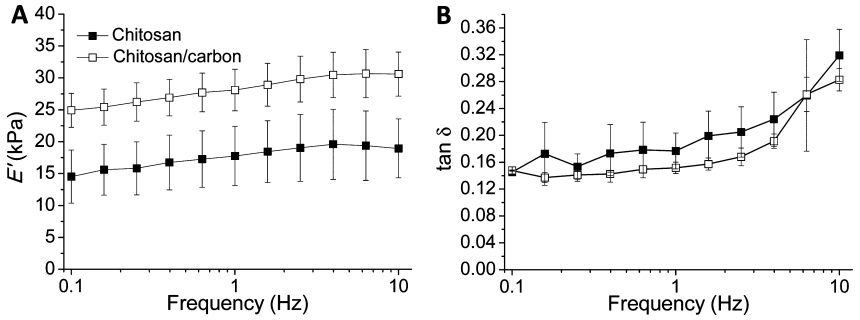

Figure 2. Dynamic mechanical properties of the scaffolds. Data are shown for cylindrical scaffolds (6 mm diameter × 4 mm thick discs) in hydrated state. (A) Storage modulus (E') and (B) loss factor (tan δ) as a function of frequency under dynamic compression solicitation. Results are expressed as means ± standard deviation ($n = 3$ for each group and time point).

(Harlan, South Easton, MA), as previously described[9] according to an institutionally approved IACUC protocol. Briefly, heart ventricles were quartered, incubated at 4 °C in a 0.06% (w/v) trypsin in Hank's Balanced Salt Solution (HBSS, Gibco, Carlsbad, CA), and subjected to a series of digestions (3−4 min, 37 °C, 150 rpm) in a 0.1% (w/v) solution of collagenase type II (Worthington Biochemical Corp., Lakewood, NJ) in HBSS. Cell suspensions from the first 4−5 digestions were collected and preplated in polystyrene culture flasks for 75 min to remove the readily adhering cardiac fibroblasts. The nonadherent cells, that are enriched for cardiac myocytes, were counted using a hemocytometer and suspended in cardiac medium (CM) consisting of high glucose Dulbecco's Modified Eagle's Medium (DMEM, Gibco) supplemented with 10% heat inactivated fetal bovine serum, as previously described.[9]

Scaffolds (6 mm diameter × 1.5 mm thick discs) were hydrated in culture medium in six-well plates and seeded with neonatal rat cardiomyocytes (5×10^6 cells in 25 μL Matrigel (Becton Dickinson, Franklin Lakes, NJ)), as described previously.[9] After 45 min, 6 mL of culture medium was added to each well. High glucose Dulbecco's modified Eagle's medium (DMEM) was used, supplemented with 10% heat-inactivated fetal bovine serum (FBS; Invitrogen, Carlsbad, CA, U.S.A.), 1% HEPES, and 1% penicillin/streptomyocin (P/S). The medium was changed every day. After 7 and 14 days, cell/constructs were removed from plates and analyzed.

Metabolic Activity. Cellular metabolism was evaluated using 3-(4,5-dimethylthiazol-2-yl)-5-(3-carboxymethoxyphenyl)-2-(4-sulfophenyl)-2*H*-tetrazolium (MTS) assay (Promega; $n = 4$). Optical density (O.D.) was calculated as the difference between the measured value of the cell-seeded groups and the cell-free controls. Optical density values from MTS assay were assessed after 7 and 14 days of culture with neonatal cardiomyocytes on chitosan and chitosan/carbon scaffolds.

Scanning Electron Microscopy (SEM). Scanning electron microscopy (SEM) was used to evaluate the scaffold morphology and infiltration of the cells. At timed intervals, constructs were removed from the plates, washed in PBS, and fixed with 2.5% glutaraldehyde for 30 min. The samples were then washed with PBS, dehydrated in a graded series of ethanol, dried by hexamethyldisilazane, mounted on aluminum stages, sputter coated with gold (Fisons Instruments, Sputter Coater SC502, U.K.), and examined with an a Leica Cambridge S360 Scanning electron microscope.

Histological Evaluation. The remaining scaffold/cell constructs were rinsed with PBS, fixed in 4% paraformaldeheyde solution embedded in paraffin, sectioned perpendicular to the scaffold diameter in 5 mm thick cross sections and stained with hematoxylin and eosin (H&E) for histological evaluation. Sections were visualized using Olympus IX81 light microscope (Center Valley, PA).

Gene Expression. The expression profiles of specific-cardiac markers: Atrial natriuretic factor (Anf or Nppa); α-myosin heavy chain (Myh6); β-myosin heavy chain (Myh7); Troponin T Type 2 (Tnnt2); Troponin C Type 1 (Tnnc1); Gata binding protein 4 (Gata4); Gap junction protein, α-1 or connexin-43 (Gja1 or Cx43); and calcium-transporting ATPase (Atp2a2 or Serca-2) were analyzed by real-time quantitative PCR.

Cell constructs were harvested after 7 and 14 days of culture to evaluate the RNA levels of cardiac genes. Constructs were disintegrated in 1 mL of Trizol using steel beads and a bead beater rotator MiniBeadBeater-8 (Biospec Products, Bartlesville, OK), and RNA was extracted using Trizol reagent according to the manufacturer's instructions. RNA quantity and purity were assessed using a NanoDrop ND-1000 spectrophotometer (NanoDrop Technologies, U.S.A.). Samples with a 260:280 ratio of 1.6 and 2.0. cDNA were prepared using Ready-To-Go You-Prime First-Strand Beads kit (GE Healthcare Life Sciences) according to the manufacturer's instructions. Primers and glyceraldehyde-3-phosphate-dehydrogenase (GAPDH) were purchased from Applied Biosystems (Foster City, CA, U.S.A.).

Real-time quantitative PCR (real time-qPCR) analysis was performed on the ABI Prism 7700 Sequence Detection Instrument (Applied Biosystems, Foster City, CA, U.S.A.). The Livak method $(_2^{-\Delta\Delta CT})$[35] was used to quantify relative and absolute expressions of each gene between chitosan/carbon scaffolds and chitosan scaffolds. Expression of cardiac specific genes was normalized to GAPDH, and data were calculated as fold change relative to the control (chitosan/carbon/cell constructs vs chitosan/cell constructs, $n = 4-5$ per group and time point).

Statistics. Results are expressed as mean ± SD, with $n = 3-5$ per group and time point. Single factor analysis of variance (ANOVA) was used to determine statistical significance within a data set. If ANOVA detected a significant difference within the data set, Tukey HSD posthoc test was used to determine significant differences between groups. Differences were considered to be significant when $p < 0.05$.

RESULTS AND DISCUSSION

Scaffold Structure. The porosity, pore interconnectivity, and pore sizes determined by μCT analysis were comparable for chitosan scaffolds and chitosan/carbon scaffolds (Table 1). Chitosan scaffolds had the void volume of 91.5 ± 0.98% and pore interconnectivity of 96.9 ± 1.3%. The pore interconnectivity of the scaffolds was maintained with the incorporation of carbon nanofibers into chitosan, with only a slight (but not statistically significant) decrease in porosity and pore size (Table 1). Overall, no significant differences in scaffold structure were observed with the addition of carbon nanofibers.

Mechanical Properties of Hydrated Scaffolds. The scaffolds were evaluated using dynamic mechanical analysis (DMA),[36] in fully hydrated state, over a range of frequencies (0.1, 0.16, 0.25, 0.40, 0.63, 1.0, 1.6, 2.5, 4.0, 6.3, and 10 Hz). The viscoelastic behavior was evaluated by measuring the storage modulus (E') and the loss factor ($\tan \delta = E''/E'$, where E'' is the viscous modulus; Figure 2). For both scaffolds, the elastic modulus increased continuously over the tested frequency range, and was at all frequencies higher for the chitosan/carbon scaffolds than pure chitosan scaffolds. At 1 Hz, a slight but significant difference was observed in the elastic moduli of chitosan and chitosan/carbon scaffolds (Table 1), and both values were in the range of those measured for muscle (8−17 kPa)[37] and myocardium in healthy rats (18 kPa),[38] indicating the ability of the scaffolds to store energy under cyclic load.

The values of the loss factor $\tan \delta$ in Figure 2 indicate that the damping properties of both scaffolds increased with frequency, and were not significantly changed by the incorporation of carbon nanofibers. In both the chitosan and chitosan/carbon scaffolds, the loss factor had values between 0.14 and 0.32, indicative of viscoelastic properties, with the viscous component of the dynamic modulus 5 times lower than the elastic modulus. In general, the values of the loss factor indicate that the scaffolds have ability to recover under cyclic loads, and that the relaxation times shortened at higher frequencies, such that the scaffolds dissipated more energy under cyclic loading. Native cardiac tissues also exhibit damping properties under cyclic loading, with hysteresis between loading−unloading stress−strain curves. For example, bovine pericardial tissue dissipates about 20% of the loading energy during loading−unloading, at frequencies of 0.1−10 Hz.[39]

Scaffold Swelling and Degradation. Material resorption is generally desired, and the degradation products must be nontoxic and readily eliminated from the body. Ideally, the degradation rate of the scaffold should correspond to the regeneration rate of the new tissue. To evaluate degradation, the scaffolds were immersed in PBS solution for 60 days under both static and agitation conditions. Chitosan is a hydrophilic polymer, and the chitosan scaffolds absorbed PBS to ∼550% of their weight and maintained this degree of swelling over 60 days of incubation (Figure 3). The lower water uptake of chitosan/carbon scaffolds was proportionate to the fraction of carbon nanofibers, which are hydrophobic, within the hydrophilic chitosan scaffold matrix (Figure 3).

Over 60 days, the structural integrity of chitosan/carbon scaffolds was maintained, without measurable loss of material due to degradation. In contrast, degradation of chitosan scaffolds without carbon was observed in our previous studies in the presence of lysozyme,[18] an enzyme ubiquitous in the human body[40,41] that degrades chitosan in vitro and in vivo.[42,43]

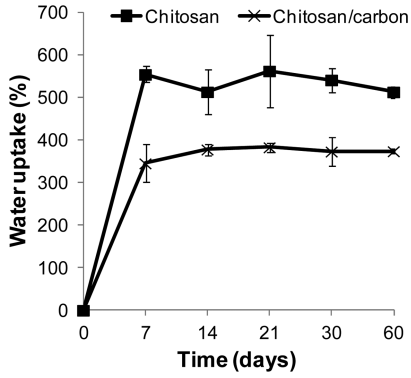

Figure 3. Swelling properties. Water uptake by the scaffolds (6 mm diameter × 1.5 mm thick cylinders) as a function of immersion time in PBS (pH 7.4, 37 °C). Data are shown as % increase in the scaffold weight, as means ± SD (n = 4 per group and time point).

In that study, lysozyme was used at concentrations similar to those found in human serum,[18] at pH 5.[44] We also investigated the in vivo degradation of chitosan scaffolds over 3 months[21] and again observed a weight loss as a function of time (3, 6, and 12 weeks).[21] Taken together, these data establish the kinetics and mechanisms of chitosan degradation and support the need for future studies evaluating the degradation of chitosan/carbon scaffolds in vivo.

Electrical Conductivity. A comparative analysis of the conductivity of the scaffolds shows that carbon nanofibers strongly improved the electrical conductivity (Table 1). The electrical conductivity of chitosan/carbon scaffolds, measured in a dry state as in previous studies,[30,31] was 9 orders of magnitude above that of chitosan scaffolds. Importantly, the electrical conductivity of chitosan/carbon scaffolds is in the same order of magnitude as the conductivity of ventricular muscle, blood, and skeletal muscle (0.03−0.6 S/m).[45]

After the scaffolds are hydrated, bulk conductivity of the bulk material is largely determined by the conductivity of liquid, so that the hydrated chitosan scaffolds markedly increased their conductivity compared with dry scaffolds (0.03 ± 0.02 S/m vs $7.4 \times 10^{-09} \pm 1.0 \times 10^{-09}$ S/m, Table 1). In the hydrated chitosan/carbon scaffolds, the conductivity was determined by both chitosan/carbon and solution (0.04 ± 0.02 S/m, Table 1). However, the microscopic conductivity of the scaffold material remains significantly higher for chitosan/carbon scaffolds. The local changes in conductivity are important as the carbon nanofibers can directly affect the membrane properties of the cardiomyocytes, by altering their resistance or capacitance even without changing the conductivity of the scaffold in its hydrated state.

Metabolic Activity. Cardiomyocytes represent only about 30% of the cells in the adult myocardium and have only a minimal ability to differentiate, proliferate, and self-renew.[46] The remaining 70% of cells are endothelial cells and fibroblasts, which have capacity to proliferate. However, cardiomyocytes are the most metabolically active cells in the human body.[47] MTS assay involves the biological reduction by viable cells of the tetrazolium compound (MTS). The MTS assay reagent is composed of MTS and the electron coupling agent phenazine methosulfate (PMS). The formazan product of MTS reduction is soluble in tissue culture medium. This reaction only takes place when mitochondrial reductase enzymes are active, and therefore, the conversion can be directly related to the viability of cells in culture.

In chitosan and chitosan/carbon scaffolds, cells were able to reduce the MTS after 7 and 14 days of culture, without significant increases in metabolic rates as a function of time (Figure 4). After 14 days of culture, the metabolic activity of the cells cultured in chitosan/carbon/cell constructs was markedly and significantly higher than in chitosan scaffolds. Importantly, cell viability was maintained throughout the duration of culture. These results can be attributed to the actual differences in cell metabolic rates, as all experiments were conducted using the same cell preparations,[9] and with efficiencies of cell seeding into the scaffolds of approximately 80%.

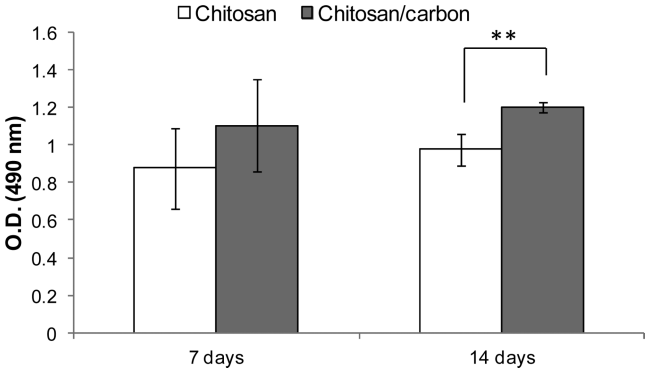

Figure 4. Metabolic activity of cardiomyocytes cultured on chitosan and chitosan/carbon cell scaffolds. Data are shown for culture of 5 million of cells per scaffold (6 mm diameter × 1.5 mm thick discs), as optical density (O.D.) values from MTS assay at 7 and 14 day time points. Results are expressed as mean ± SD (n = 4 per group and time point). (**) Indicates a significant difference (p < 0.01) between groups at the same time point.

Microstructure. Scaffolds for cardiac applications should have an interconnected structure for cell infiltration, and appropriate porosity and pore dimensions allowing high densities of seeded cells, vascularization, and effective transport of nutrients and oxygen. Myocardial cells have dimensions in the range of 10−100 μm,[48] and the pore sizes in seeded scaffolds ranged from ∼120−150 μm, as measured by SEM and histology. Morphological observation by SEM indicated homogeneous dispersion of carbon nanofibers throughout chitosan matrix (Figure 5). SEM images show highly porous scaffolds with pores infiltrated with cells after 7 and 14 days of culture, corroborating the results of μCT that showed high void volumes and high interconnectivity of the pores (Table 1).

Histomorphology. Histological cross sections of chitosan and chitosan/carbon scaffolds cultured with cardiomyocytes for 7 and 14 days (Figure 6) were consistent with the porosity, interconnectivity and size of pores measured by μCT. The cellular infiltration throughout the scaffolds was evident (Figure 6). The scaffold pores were filled with cells and well distributed throughout the scaffold volume. No significant differences in cell infiltration were observed between chitosan and chitosan/carbon scaffolds. Histological and SEM evaluations indicate that the cells assume elongated shape and start to align with each other, suggesting the need for more detailed and quantitative assessment in further studies.

Gene Expression (Real Time-qPCR). Cardiac gene expression profiles were analyzed for cardiomyocytes cultured in chitosan and chitosan/carbon scaffolds (Table 2), to evaluate the effect of carbon nanofibers on the expression of specific-cardiac genes. After 7 days of culture, all genes were overexpressed in cells on chitosan/carbon scaffolds, with the exception of Anf. Specifically, the expression of Tnnc1 and Cx43 increased 2- and 2.6-fold, respectively. The highest gene expression after 7 days of culture was observed for cardiac troponin Tnnc1 (important for contractile function in muscle tissue[49]) and Cx43 (important for conduction of electrical signals)[50−52]

Functional neonatal cardiomyocytes communicate by electrical impulses through gap junctions. This ability was enhanced

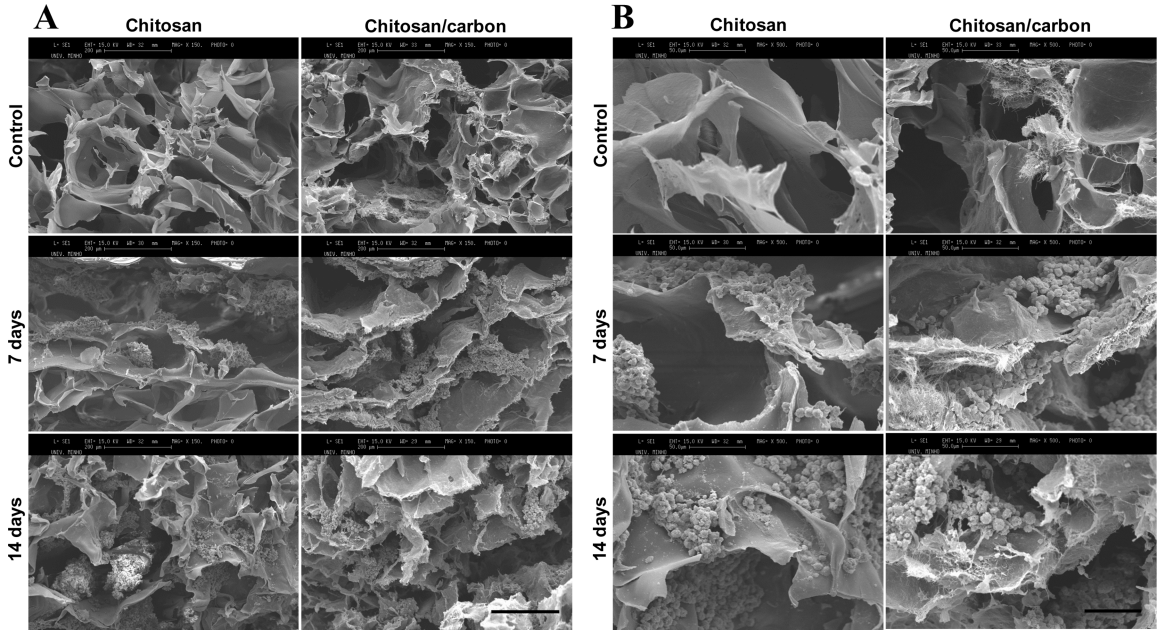

Figure 5. Scaffold ultrastructure. SEM images of the cross sections of chitosan and chitosan/carbon scaffolds without cells (control) and after 7 and 14 days of culture with neonatal cardiomyocytes. Images are presented at 150× (A) and 500× (B) magnification. The scale bar is 200 (A) and 50 μm (B).

dx.doi.org/10.1021/bm401679q | Biomacromolecules 2014, 15, 635−643

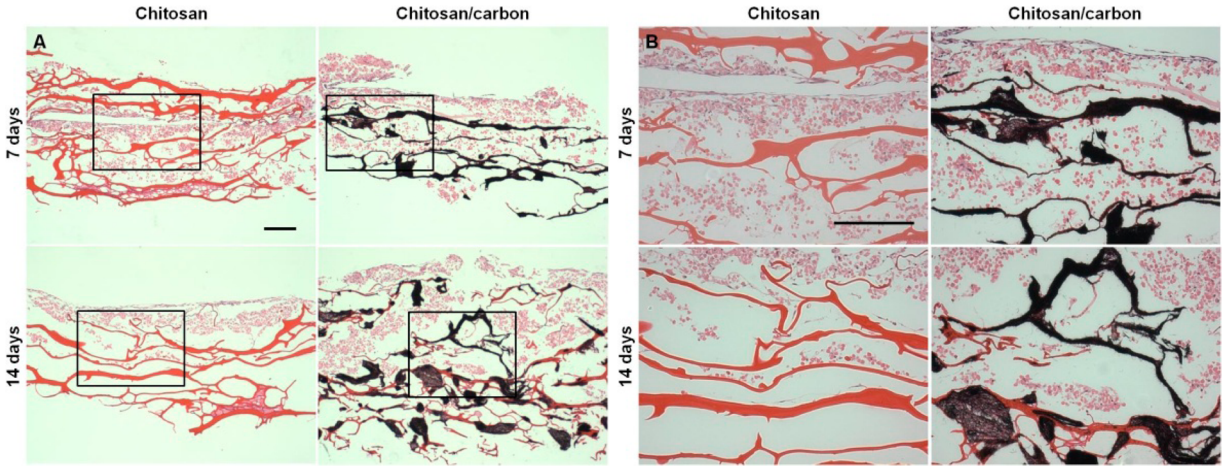

Figure 6. Histomorphology of tissue constructs. Representative histological sections of chitosan and chitosan/carbon/cell constructs after 7 and 14 days of culture stained with H&E. The images show the infiltration of cells throughout the scaffolds and are presented at 4× (A) and 10× (B) magnification. The scale bar is 200 μm for all images.

Table 2. Genes Differentially Expressed in Cardiomyocytes in the Presence of Carbon (n = 4–5)

gene	short name	function	fold change over control		ref.
			7 days	14 days	
atrial natriuretic factor	Anf or Nppa	marker of cardiomyocytes differentiation; protein secreted by heart muscle	1	4	53
Myosin heavy chain	Myh6 or Mhc-a	transcript levels start increasing, and, by postnatal day 3, is upregulated in both the right and the left ventricle	1.5	5.8	56
Myosin heavy chain	Myh7 or Mhc-β	expresses primarily in the heart	1.2	4.4	57
Troponin T type 2	Tnnt2 or cTnT	important in the structure of muscle tissue; play a role in contraction of muscle cells	1.6	2	49, 58
Troponin C type 1	Tnnc1		2	4	
Gata4	Gata4	critical regulator of cardiac gene expression; controls embryonic development, modulating cardiomyocytes differentiation; regulator of postnatal heart function	1.4	2.6	54, 55, 59, 60
gap junction α-1 or connexin 43	Cx43 or Gja1	main constituent of cardiomyocytes gap junctions and essential for cell–cell coupling; essential for structural and electrical connectivity of cardiac tissue	2.6	3.8	61, 62
calcium-transporting ATPase	Atpa2a2 or Serca2	intracellular pumps located in the sarcoplasmic or endoplasmic reticula of muscle cells and reduced activity of this gene is a hallmark of heart failure	1.7	4	63

by the presence of carbon nanofibers in chitosan scaffolds, as evidenced by elevated expression of Cx43 after 7 days (Figure 7). The higher Cx43 level on day 7, without electrical stimulation, suggests that the carbon nanofibers affect physiology independently of possible complementary effects of the external electrical field. Notably, this high expression was maintained and slightly (but not significantly) increased by day 14 of culture (Figure 7, Table 2).

Significant increases were also observed in the expression of Anf, Myh6, Myh7, Tnnc1, Gata4, and Atpa2a genes over time (Figure 7). Atrial natriuretic factor (Anf) is a powerful vasodilator, a marker of cardiomyocyte differentiation,[53] and a protein secreted by heart muscle cells was overexpressed after 14 days ($p < 0.01$). Gata4, a survival factor for differentiated cardiomyocytes and an important regulator of postnatal heart function[54,55] was also significantly upregulated ($p < 0.01$) after 14 days (Figure 7). The expression and activity of ATPase 2a has been observed to decrease in cardiomyocytes in a failing heart, and the overexpression Atpa2a could restore the cardiac function in heart failure by improving calcium handling in the cardiomyocytes.[55] Significant increase in the expression of ATP2a2 was observed in chitosan/carbon scaffolds with time in culture (Figure 7), with 4-fold higher expression relatively to control (chitosan scaffolds) after 14 days of culture (Figure 7, Table 2).

Real time qPCR thus confirms that the presence of carbon nanofibers in chitosan scaffolds enhanced the cardiogenic phenotype and expression of cardiac markers after 14 days, without external electrical stimulation. In future studies, these data will be complemented by analysis of cardiac-specific proteins in engineered cardiac constructs. Given that the macroscopic conductivity of the scaffolds in their hydrated state was not significantly different between chitosan/carbon and chitosan scaffolds, the enhanced conductivity at the microscopic scale (at the level of carbon nanofibers) clearly played a role in enhancing gene expression, possibly through microscopic gradients in voltage and currents around the cells.

CONCLUSIONS

We describe electrically conductive composite scaffolds based on chitosan, designed to have mechanical properties similar to those of cardiac muscle, and to provide local increases (by 9 orders of magnitude) in electrical conductivity by addition of carbon nanofibers. The carbon/chitosan scaffolds supported

dx.doi.org/10.1021/bm401679q | Biomacromolecules 2014, 15, 635–643

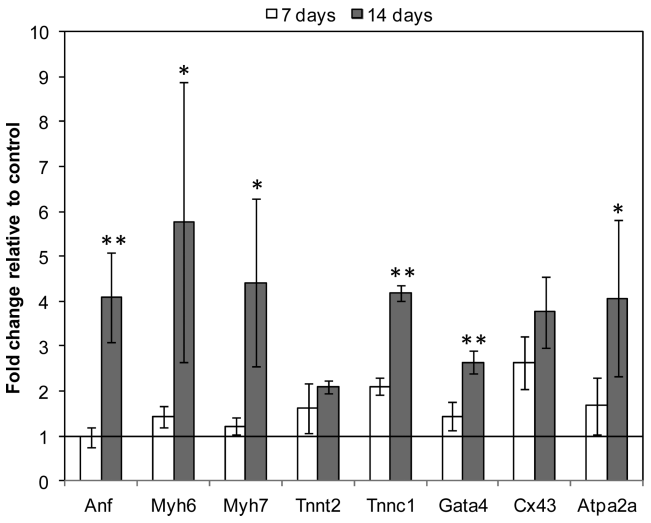

Figure 7. Gene expression. Data are shown for real time-qPCR analysis of cardiomyocytes cultured on chitosan/carbon scaffolds for 7 and 14 days vs control samples (chitosan scaffolds cultured using the same conditions). Data are shown as fold change in gene expression relatively to control (chitosan/carbon/cell constructs vs chitosan/cell constructs) and are expressed as means ± SD (n = 4−5 per group and time point). (**) Indicates a significant difference ($p < 0.01$) and (*) indicates a significant difference ($p < 0.05$) for the same gene as a function of time.

cultivation of cardiac cells and enhanced cardiogenic properties without exogenous electrical stimulation. In the presence of carbon nanofibers, cardiomyocytes were able to adhere and survive for up to 14 days, and elevate their metabolic activity and expression of cardiac genes. Gene expression profiling showed upregulation of Tnnc1 and Cx43 in chitosan/carbon/cell constructs after 7 days of culture and all measured cardiac-specific genes after 14 days of culture. Looking forward, future studies should focus on spontaneous beating and functionality of cardiac cells in these scaffolds and mapping of the electrical signal transmission.

AUTHOR INFORMATION

Corresponding Author

*E-mail: gv2131@columbia.edu.

Notes

The authors declare no competing financial interest.

ACKNOWLEDGMENTS

Funding for this work was provided by the "Fundação para a Ciência e Tecnologia" (Postdoctoral Grant SFRH/BPD/66897/2009 to A.M.M. financed by POPH - QREN − Advanced Formation, cofinanced by Social European Fund and National Fund from MCTES) and NIH (Grants EB002520 and HL076485 to G.V.-N.). The authors thank Dr. Arantza Villasante and Dr. Kara Spiller (Columbia University) for their help with qPCR experiments and data analysis, and Prof. Senentxu Lanceros-Mendez and Catarina Lopes (University of Minho) for their assistance with the electrical conductivity measurements.

REFERENCES

(1) Shin, M.; Ishii, O.; Sueda, T.; Vacanti, J. P. Contractile cardiac grafts using a novel nanofibrous mesh. *Biomaterials* **2004**, *25*, 3717−3723.

(2) Leor, J.; Landa, N.; Cohen, S. Renovation of the injured heart with myocardial tissue engineering. *Expert Rev. Cardiovasc. Ther.* **2006**, *4*, 239−252.

(3) Yang, M. C.; Wang, S. S.; Chou, N. K.; Chi, N. H.; Huang, Y. Y.; Chang, Y. L.; Shieh, M. J.; Chung, T. W. The cardiomyogenic differentiation of rat mesenchymal stem cells on silk fibroin-polysaccharide cardiac patches in vitro. *Biomaterials* **2009**, *30*, 3757−3765.

(4) Barsotti, M. C.; Felice, F.; Balbarini, A.; Di Stefano, R. Fibrin as a scaffold for cardiac tissue engineering. *Biotechnol. Appl. Biochem.* **2011**, *58*, 301−310.

(5) Zhang, T.; Wan, L. Q.; Xiong, Z.; Marsano, A.; Maidhof, R.; Park, M.; Yan, Y. N. A.; Vunjak-Novakovic, G. Channelled scaffolds for engineering myocardium with mechanical stimulation. *J. Tissue Eng. Regener. Med.* **2012**, *6*, 748−756.

(6) Patra, C.; Talukdar, S.; Novoyatleva, T.; Velagala, S. R.; Muhlfeld, C.; Kundu, B.; Kundu, S. C.; Engel, F. B. Silk protein fibroin from Antheraea mylitta for cardiac tissue engineering. *Biomaterials* **2012**, *33*, 2673−2680.

(7) Tian, B. Z.; Liu, J.; Dvir, T.; Jin, L. H.; Tsui, J. H.; Qing, Q.; Suo, Z. G.; Langer, R.; Kohane, D. S.; Lieber, C. M. Macroporous nanowire nanoelectronic scaffolds for synthetic tissues. *Nat. Mater.* **2012**, *11*, 986−994.

(8) Zorlutuna, P.; Elsheikh, A.; Hasirci, V. Nanopatterning of collagen scaffolds improve the mechanical properties of tissue engineered vascular grafts. *Biomacromolecules* **2009**, *10*, 814−821.

(9) Radisic, M.; Park, H.; Shing, H.; Consi, T.; Schoen, F. J.; Langer, R.; Freed, L. E.; Vunjak-Novakovic, G. Functional assembly of engineered myocardium by electrical stimulation of cardiac myocytes cultured on scaffolds. *Proc. Natl. Acad. Sci. U.S.A.* **2004**, *101*, 18129−18134.

(10) Tandon, N.; Marsano, A.; Maidhof, R.; Wan, L.; Park, H.; Vunjak-Novakovic, G. Optimization of electrical stimulation parameters for cardiac tissue engineering. *J. Tissue Eng. Regener. Med.* **2011**, *5*, E115−E125.

(11) Dvir, T.; Timko, B. P.; Brigham, M. D.; Naik, S. R.; Karajanagi, S. S.; Levy, O.; Jin, H. W.; Parker, K. K.; Langer, R.; Kohane, D. S. Nanowired three-dimensional cardiac patches. *Nat. Nanotechnol.* **2011**, *6*, 720−725.

(12) Maidhof, R.; Tandon, N.; Lee, E. J.; Luo, J. W.; Duan, Y.; Yeager, K.; Konofagou, E.; Vunjak-Novakovic, G. Biomimetic perfusion and electrical stimulation applied in concert improved the assembly of engineered cardiac tissue. *J. Tissue Eng. Regener. Med.* **2012**, *6*, e12−e23.

(13) Fernandes, E. G. R.; Zucolotto, V.; De Queiroz, A. A. A. Electrospinning of hyperbranched poly-L-lysine/polyaniline nanofibers for application in cardiac tissue engineering. *J. Macromol. Sci., Part A* **2010**, *47*, 1203−1207.

(14) Stout, D. A.; Basu, B.; Webster, T. J. Poly(lactic-*co*-glycolic acid): Carbon nanofiber composites for myocardial tissue engineering applications. *Acta Biomater.* **2011**, *7*, 3101−3112.

(15) You, J. O.; Rafat, M.; Ye, G. J. C.; Auguste, D. T. Nanoengineering the heart: conductive scaffolds enhance Connexin 43 expression. *Nano Lett.* **2011**, *11*, 3643−3648.

(16) Borriello, A.; Guarino, V.; Schiavo, L.; Alvarez-Perez, M. A.; Ambrosio, L. Optimizing PANi doped electroactive substrates as patches for the regeneration of cardiac muscle. *J. Mater. Sci.: Mater. Med.* **2011**, *22*, 1053−1062.

(17) Stout, D. A.; Yoo, J.; Santiago-Miranda, A. N.; Webster, T. J. Mechanisms of greater cardiomyocyte functions on conductive nanoengineered composites for cardiovascular applications. *Int. J. Nanomed.* **2012**, *7*, 5653−5669.

(18) Martins, A. M.; Santos, M. I.; Azevedo, H. S.; Malafaya, P. B.; Reis, R. L. Natural origin scaffolds with in situ pore forming capability for bone tissue engineering applications. *Acta Biomater.* **2008**, *4*, 1637−1645.

(19) Martins, A. M.; Pham, Q. P.; Malafaya, P. B.; Raphael, R. M.; Kasper, F. K.; Reis, R. L.; Mikos, A. G. "Smart" and stimulus responsive chitosan-based scaffolds/cells for bone tissue engineering:

Influence of lysozyme upon scaffold degradation and osteogenic differentiation of cultured marrow stromal cells induced by cap coatings. *Tissue Eng., Part A* **2008**, *14*, 795−795.
(20) Martins, A. M.; Alves, C. M.; Kasper, F. K.; Mikos, A. G.; Reis, R. L. Responsive and in situ-forming chitosan scaffolds for bone tissue engineering applications: an overview of the last decade. *J. Mater. Chem.* **2010**, *20*, 1638−1645.
(21) Martins, A. M.; Kretlow, J. D.; Costa-Pinto, A. R.; Malafaya, P. B.; Fernandes, E. M.; Neves, N. M.; Alves, C. M.; Mikos, A. G.; Kasper, F. K.; Reis, R. L. Gradual pore formation in natural origin scaffolds throughout subcutaneous implantation. *J. Biomed. Mater. Res., A* **2012**, *100*, 599−612.
(22) Madihally, S. V.; Matthew, H. W. Porous chitosan scaffolds for tissue engineering. *Biomaterials* **1999**, *20*, 1133−1142.
(23) Ueno, H.; Mori, T.; Fujinaga, T. Topical formulations and wound healing applications of chitosan. *Adv. Drug Delivery Rev.* **2001**, *52*, 105−115.
(24) Hoekstra, A.; Struszczyk, H.; Kivekas, O. Percutaneous microcrystalline chitosan application for sealing arterial puncture sites. *Biomaterials* **1998**, *19*, 1467−1471.
(25) Kumar, M. N. V. R. A review of chitin and chitosan applications. *React. Funct. Polym.* **2000**, *46*, 1−27.
(26) Khor, E. Chitin: a biomaterial in waiting. *Curr. Opin. Solid State Mater. Sci.* **2002**, *6*, 313−317.
(27) Lu, W. N.; Lu, S. H.; Wang, H. B.; Li, D. X.; Duan, C. M.; Liu, Z. Q.; Hao, T.; He, W. J.; Xu, B.; Fu, Q.; Song, Y. C.; Xie, X. H.; Wang, C. Y. Functional improvement of infarcted heart by co-injection of embryonic stem cells with temperature-responsive chitosan hydrogel. *Tissue Eng., Part A* **2009**, *15*, 1437−1447.
(28) Wang, H. B.; Zhang, X. L.; Li, Y. M.; Ma, Y. T.; Zhang, Y.; Liu, Z. G.; Zhou, J.; Lin, Q. X.; Wang, Y. M.; Duan, C. M.; Wang, C. Y. Improved myocardial performance in infarcted rat heart by co-injection of basic fibroblast growth factor with temperature-responsive Chitosan hydrogel. *J. Heart Lung Transpl.* **2010**, *29*, 881−887.
(29) Liu, Z. Q.; Wang, H. B.; Wang, Y.; Lin, Q. X.; Yao, A. N.; Cao, F.; Li, D. X.; Zhou, J.; Duan, C. M.; Du, Z. Y.; Wang, Y. M.; Wang, C. Y. The influence of chitosan hydrogel on stem cell engraftment, survival and homing in the ischemic myocardial microenvironment. *Biomaterials* **2012**, *33*, 3093−3106.
(30) Vamvakaki, V.; Tsagaraki, K.; Chaniotakis, N. Carbon nanofiber-based glucose biosensor. *Anal. Chem.* **2006**, *78*, 5538−5542.
(31) Wu, L.; Lei, J. P.; Zhang, X. J.; Ju, H. X. Biofunctional nanocomposite of carbon nanofiber with water-soluble porphyrin for highly sensitive ethanol biosensing. *Biosens. Bioelectron.* **2008**, *24*, 644−649.
(32) Tran, P. A.; Zhang, L. J.; Webster, T. J. Carbon nanofibers and carbon nanotubes in regenerative medicine. *Adv. Drug Delivery Rev.* **2009**, *61*, 1097−1114.
(33) Wang, S. F.; Shen, L.; Zhang, W. D.; Tong, Y. J. Preparation and mechanical properties of chitosan/carbon nanotubes composites. *Biomacromolecules* **2005**, *6*, 3067−3072.
(34) Lau, C.; Cooney, M. J.; Atanassov, P. Conductive macroporous composite chitosan-carbon nanotube scaffolds. *Langmuir* **2008**, *24*, 7004−7010.
(35) Livak, K. J.; Schmittgen, T. D. Analysis of relative gene expression data using real-time quantitative PCR and the 2(T)(-$\delta\delta$C) method. *Methods* **2001**, *25*, 402−408.
(36) Mano, J. C.;Reis, R. L.;Cunha, A. M. Dynamic Mechanical Analysis in Polymers for Biomedical Applications. In *Polymer Based Systems on Tissue Engineering, Replacement and Regeneration*; Reis, R. L., Cohn, D, Eds.; Dordrecht: Kluwer, 2002; p 139−164.
(37) Engler, A. J.; Sen, S.; Sweeney, H. L.; Discher, D. E. Matrix elasticity directs stem cell lineage specification. *Cell* **2006**, *126*, 677−689.
(38) Berry, M. F.; Engler, A. J.; Woo, Y. J.; Pirolli, T. J.; Bish, L. T.; Jayasankar, V.; Morine, K. J.; Gardner, T. J.; Discher, D. E.; Sweeney, H. L. Mesenchymal stem cell injection after myocardial infarction improves myocardial compliance. *Am. J. Physiol.* **2006**, *290*, H2196−H2203.
(39) Mavrilas, D.; Sinouris, E. A.; Vynios, D. H.; Papageorgakopoulou, N. Dynamic mechanical characteristics of intact and structurally modified bovine pericardial tissues. *J. Biomech.* **2005**, *38*, 761−768.
(40) Hankiewi., J.; Swiercze., E. Lysozyme in human body fluids. *Clin. Chim. Acta* **1974**, *57*, 205−209.
(41) Porstmann, B.; Jung, K.; Schmechta, H.; Evers, U.; Pergande, M.; Porstmann, T.; Kramm, H. J.; Krause, H. Measurement of lysozyme in human body fluids: comparison of various enzyme-immunoassay techniques and their diagnostic application. *Clin. Biochem.* **1989**, *22*, 349−355.
(42) Varum, K. M.; Myhr, M. M.; Hjerde, R. J. N.; Smidsrod, O. In vitro degradation rates of partially N-acetylated chitosans in human serum. *Carbohydr. Res.* **1997**, *299*, 99−101.
(43) Tomihata, K.; Ikada, Y. In vitro and in vivo degradation of films of chitin and its deacetylated derivatives. *Biomaterials* **1997**, *18*, 567−575.
(44) Martins, A. M.; Pereira, R. C.; Leonor, I. B.; Azevedo, H. S.; Reis, R. L. Chitosan scaffolds incorporating lysozyme into CaP coatings produced by a biomimetic route: A novel concept for tissue engineering combining a self-regulated degradation system with in situ pore formation. *Acta Biomater.* **2009**, *5*, 3328−3336.
(45) Potse, M.; Dube, B.; Vinet, A. Cardiac anisotropy in boundary-element models for the electrocardiogram. *Med. Biol. Eng. Comput.* **2009**, *47*, 719−729.
(46) Nag, A. C. Study of non-muscle cells of the adult mammalian heart: a fine-structural analysis and distribution. *Cytobios* **1980**, *28*, 41−61.
(47) Severs, N. J. The cardiac muscle cell. *Bioessays* **2000**, *22*, 188−199.
(48) Davis, M. E.; Hsieh, P. C.; Grodzinsky, A. J.; Lee, R. T. Custom design of the cardiac microenvironment with biomaterials. *Circ. Res.* **2005**, *97*, 8−15.
(49) Ling-Ling, E.; Zhao, Y. S.; Guo, X. M.; Wang, C. Y.; Jiang, H.; Li, J.; Duan, C. M.; Song, Y. Enrichment of cardiomyocytes derived from mouse embryonic stem cells. *J. Heart Lung Transpl.* **2006**, *25*, 664−674.
(50) Lo, C. W. Role of gap junctions in cardiac conduction and development: insights from the connexin knockout mice. *Circ. Res.* **2000**, *87*, 346−348.
(51) Vaidya, D.; Tamaddon, H. S.; Lo, C. W.; Taffet, S. M.; Delmar, M.; Morley, G. E.; Jalife, J. Null mutation of connexin43 causes slow propagation of ventricular activation in the late stages of mouse embryonic development. *Circ. Res.* **2001**, *88*, 1196−1202.
(52) Kostin, S.; Dammer, S.; Hein, S.; Klovekorn, W. P.; Bauer, E. P.; Schaper, J. Connexin 43 expression and distribution in compensated and decompensated cardiac hypertrophy in patients with aortic stenosis. *Cardiovasc. Res.* **2004**, *62*, 426−436.
(53) Temsah, R.; Nemer, M. GATA factors and transcriptional regulation of cardiac natriuretic peptide genes. *Regul. Pept.* **2005**, *128*, 177−185.
(54) Hosoda, T.; Monzen, K.; Hiroi, Y.; Oka, T.; Takimoto, E.; Yazaki, Y.; Nagai, R.; Komuro, I. A novel myocyte-specific gene Midori promotes the differentiation of P19CL6 cells into cardiomyocytes. *J. Biol. Chem.* **2001**, *276*, 35978−35989.
(55) Aries, A.; Paradis, P.; Lefebvre, C.; Schwartz, R. J.; Nemer, M. Essential role of GATA-4 in cell survival and drug-induced cardiotoxicity. *Proc. Natl. Acad. Sci. U.S.A.* **2004**, *101*, 6975−6980.
(56) Zammit, P. S.; Kelly, R. G.; Franco, D.; Brown, N.; Moorman, A. F.; Buckingham, M. E. Suppression of atrial myosin gene expression occurs independently in the left and right ventricles of the developing mouse heart. *Dev. Dynam.* **2000**, *217*, 75−85.
(57) Bin, Z.; Sheng, L. G.; Gang, Z. C.; Hong, J.; Jun, C.; Bo, Y.; Hui, S. Efficient cardiomyocyte differentiation of embryonic stem cells by bone morphogenetic protein-2 combined with visceral endoderm-like cells. *Cell Biol. Int.* **2006**, *30*, 769−776.
(58) Saggin, L.; Ausoni, S.; Gorza, L.; Sartore, S.; Schiaffino, S. Troponin-T switching in the developing rat-heart. *J. Biol. Chem.* **1988**, *263*, 18488−18492.

(59) Kodama, H.; Inoue, T.; Watanabe, R.; Yasuoka, H.; Kawakami, Y.; Ogawa, S.; Ikeda, Y.; Mikoshiba, K.; Kuwana, M. Cardiomyogenic potential of mesenchymal progenitors derived from human circulating CD14(+) monocytes. *Stem Cells Dev.* **2005**, *14*, 676−686.
(60) Oka, T.; Maillet, M.; Watt, A. J.; Schwartz, R. J.; Aronow, B. J.; Duncan, S. A.; Molkentin, J. D. Cardiac-specific deletion of Gata4 reveals its requirement for hypertrophy, compensation, and myocyte viability. *Circ. Res.* **2006**, *98*, 837−845.
(61) Dang, X. T.; Doble, B. W.; Kardami, E. The carboxy-tail of connexin-43 localizes to the nucleus and inhibits cell growth. *Mol. Cell. Biochem.* **2003**, *242*, 35−38.
(62) Boengler, K.; Heusch, G.; Schulz, R. Connexin 43 and ischemic preconditioning: effects of age and disease. *Exp. Gerontol.* **2006**, *41*, 485−488.
(63) Kawase, Y.; Ly, H. Q.; Prunier, F.; Lebeche, D.; Shi, Y. F.; Jin, H. W.; Hadri, L.; Yoneyama, R.; Hoshino, K.; Takewa, Y.; Sakata, S.; Peluso, R.; Zsebo, K.; Gwathmey, J. K.; Tardif, J. C.; Tanguay, J. F.; Hajar, R. J. Reversal of cardiac dysfunction after long-term expression of SERCA2a by gene transfer in a pre-clinical model of heart failure. *J. Am. Coll. Cardiol.* **2008**, *51*, 1112−1119.